ELSEVIER

Materials Science and Engineering B 135 (2006) 25–29

MATERIALS SCIENCE & ENGINEERING B

www.elsevier.com/locate/mseb

Co/CoAl/Co trilayer fabrication using spontaneous intermixing of Co and Al: Molecular dynamics simulation

Sang-Pil Kim [a], Yong-Chae Chung [a,*], Seung-Cheol Lee [b], Kwang-Ryeol Lee [b], Deok-Soo Kim [c]

[a] *Division of Materials Science and Engineering, Hanyang University, Seoul 133-791, South Korea*
[b] *Future Technology Research Division, KIST, Cheongryang, Seoul 130-650, South Korea*
[c] *VDRC, Department of Industrial Engineering, Hanyang University, Seoul 133-791, South Korea*

Received 13 February 2006; received in revised form 5 August 2006; accepted 9 August 2006

Abstract

A multilayer structure was simulated using spontaneous intermixing of Co and Al in epitaxial Co(1 1 $\bar{2}$ 0)/CoAl/Co(1 1 $\bar{2}$ 0) structures. When Al atoms with 0.1 eV energy were deposited on Co(1 1 $\bar{2}$ 0), an Al(1 0 0) thin film was grown without any intermixing. Interestingly, during subsequent deposition of Co atoms on the grown Al(1 0 0) thin film, an intermixed layer of ordered CoAl structure was spontaneously formed and a highly oriented Co(1 1 $\bar{2}$ 0) crystalline phase was grown above the intermixed region. From the calculations of nearest neighbor distributions, various compositions of Co_xAl_{1-x} structures were observed in the mixed region.

Keywords: Multilayer; Interface mixing; Co–Al; Molecular dynamics

1. Introduction

Nano-scale multilayers with various interesting structural and electro-magnetic properties have been employed in many applications. Specifically, magnetic devices consisting of magnetic and nonmagnetic alternating layers have generated a great deal of interest because of their wide technological applicability [1–6]. In a magnetic device utilizing giant magneto-resistance (GMR) property, the performance is largely dependent on the characteristics of the interface region between thin film layers. The structure is generally composed of two ferromagnetic layers with a nonmagnetic layer between them. The spin polarization at the junction is critically affected by the crystal structure of the thin films, and slight intermixing at the interfaces is generally known to result in enormous problems with the magnetic properties of the device [7].

Previously, we have investigated deposition behavior in the Co–Al system using molecular dynamics (MD) simulation. Specifically, a surface alloy was reported to be formed for various Al surface orientations even when the incident energy of the Co atom was only 0.1 eV, and an ordered B2 CoAl crystalline structure was formed spontaneously on the Al(1 0 0) surface [8]. However, in the case of Al deposition on a Co substrate, no mixing was observed at the interface [9]. The different growth behaviors could be explained in terms of the kinetic energy barrier for intermixing and the degree of local acceleration experienced by the depositing atoms near the substrate surface [10,11].

As the scale goes down to an atomic level, the lattice mismatch and the stacking sequence at the interface become essential issues for various thin film growth processes [12]. In this point of view, the Co-based system is a very attractive one because of the expression of magnetic properties with various combinations of feasible structures. It is worth mentioning that the epitaxial growth of Co(1 1 $\bar{2}$ 0) films on Mo(1 0 0) or Cr(1 0 0) has been reported, [13,14] and the correlation between the hcp(1 1 $\bar{2}$ 0) and cubic(1 0 0) orientation was successfully explained [15]. The intermetallic CoAl film was suggested as a nonmagnetic layer for electro-magnetic devices [16,17] utilizing the peculiar electro-magnetic property of the B2 CoAl intermetallic compound [18]. In connection with the Co–Al multilayer system, it is interesting to note that the previous experimental results have focused on demonstrating the influence of the deposition process on the structural and magnetic properties [19,20].

* Corresponding author. Tel.: +82 2 2220 0507; fax: +82 2 2281 5308.
E-mail address: yongchae@hanyang.ac.kr (Y.-C. Chung).

0921-5107/$ – see front matter © 2006 Elsevier B.V. All rights reserved.
doi:10.1016/j.mseb.2006.08.027

Table 1
Properties of Al, B2 CoAl and Co predicted by EAM potentials employed in this study in comparison with experimental data from literatures

Property	Co		B2 CoAl		Al	
	EAM [22]	Expt.[a]	EAM [24]	Expt.[b]	EAM [23]	Expt.[a]
a_0 (Å)	2.507	2.51	2.86	2.86	4.05	4.05
E_{coh} (eV)	4.39	4.39	4.47	4.45	3.36	3.36
c_{11} (eV/Å^3)	1.9944	1.912	1.41	1.68	1.07	1.14
c_{12} (eV/Å^3)	1.0368	1.031	0.91	0.67	0.652	0.619
c_{13} (eV/Å^3)	0.6373	0.638	–	–	–	–
c_{33} (eV/Å^3)	2.3321	2.231	–	–	–	–
c_{44} (eV/Å^3)	0.5144	0.469	0.72	0.87	0.322	0.316

[a] Experimental data from Ref. [25].
[b] Experimental data from Ref. [26].

In this study, a novel process for the fabrication of a Co/CoAl/Co trilayer using spontaneous intermixing between Co and Al is proposed. The deposition and mixing behavior was analyzed for the individual cases of Co/Al and Al/Co with crystallographic considerations at the interface. The molecular dynamics simulation method was employed to obtain a detailed picture of the thin film growth behavior. Quantitative structural analysis of each layer of the thin film structure was performed by the calculating the distribution of nearest neighbor atoms.

2. Calculation procedures

The embedded-atom method (EAM) based on interatomic potentials was utilized in this study [21]. Specifically, the potential developed by Pasianot and Savino for Co–Co [22], and the Voter and Chen potential for Al–Al were employed [23]. The pair potential of Co–Al was formulated by a linear combination of the effective pair interactions [24]. Each of the adopted potentials employed showed good agreement with the experimental values for pure elements as well as intermetallic compounds of the constituent atoms as shown in Table 1.

The substrate was composed of 3840 Co atoms with the surface consisting of the (1 1 $\bar{2}$ 0) plane containing 192 atoms. The dimensions of the substrate were 6.95 nm × 2.44 nm × 2.51 nm thick in the z direction normal to the substrate. Periodic boundary conditions were utilized in the x and y directions. The position of the bottom-most 5 layers was fixed and the remaining 15 layers of the substrate were kept at 300 K using the atom-velocity-rescaling method. The adatoms were randomly positioned in the x–y plane at a distance sufficiently far from the substrate surface to be considered as free atoms. The initial velocity of each incident atom can be calculated from the incident energy by the following expression:

$$V_{\text{adatom}} = \sqrt{\frac{2K_{\text{i}}}{M}} \quad (1)$$

where K_{i} represents the incident kinetic energy and M is the atomic mass. The MD time step was set to 1 femto-second (fs). From the calculations of single atom deposition, the moment an adatom collides with the substrate, the energy of adatom found to be spreaded very quickly to neighboring atoms and disappeared in less than 2 ps. Therefore, considering the safety factor, the total evolution time for a single atom was set to 5 ps (deposition rate 1.306×10^{-1} nm/ns). This rate is within the range between 1.7×10^{-9} and 1.7×10^{-1} nm/ns, in which the vacancy concentration is reported to be almost independent of deposition rate at 300 K [27]. The XMD 2.5.32 code was employed for the corresponding molecular dynamics simulation [28].

3. Results and discussion

The deposition simulation performed for three monolayers (ML) of Al adatoms with the low incident energy of 0.1 eV on a Co(1 1 $\bar{2}$ 0) substrate resulted in ordered fcc Al(1 0 0) films on the Co(1 1 $\bar{2}$ 0) substrate. The formation of well ordered fcc Al films on a Co(1 1 $\bar{2}$ 0) surface could be reasonably explained on the basis that the distance between the Co substrate atoms along [0 0 0 1] direction is 0.405 nm, which is almost identical to the lattice constant of fcc Al, 0.404 nm (Fig. 1).

Twenty ML of Co atoms were subsequently deposited with a relatively high incident energy of 3.0 and 5.0 eV on the ordered fcc Al(1 0 0) layers. (Fig. 2). In both incident energy cases, the well ordered Al(1 0 0) films apparently disappeared and most of Al atoms seemed to be mixed with deposited Co atoms. As shown in Fig. 1, the interatomic distance of B2 CoAl structure is 0.404 nm along the [0 1 1] direction, which is less than a 0.1% lattice mismatch with the lattice constant of fcc Al(1 0 0). In addition, the similar crystallographic symmetry and the strong affinity between Co and Al atoms would further enhance the epitaxial formation of well-intermixed alloys on the Co(1 1 $\bar{2}$ 0) surface.

Above the intermixed region, the layers of Co with (1 1 $\bar{2}$ 0) surface orientation were found to be grown without any lattice distortion. The perfect lattice match between Co(1 1 $\bar{2}$ 0) and B2 CoAl(1 0 0) can be clearly seen in Fig. 1. During the deposition process, it is noteworthy that active intermixing only occurred in the case of the Co deposition on the Al surface and not in the case of Al deposition on a Co surface in spite of a strong chemical affinity between Co and Al. The difference in the behavior of intermixing could be explained by the observation that in the Al/Co(1 0 0) case a much higher energy barrier must be overcome for the incorporation of adatoms into the Co substrate compared to the Co/Al(1 0 0) case [11].

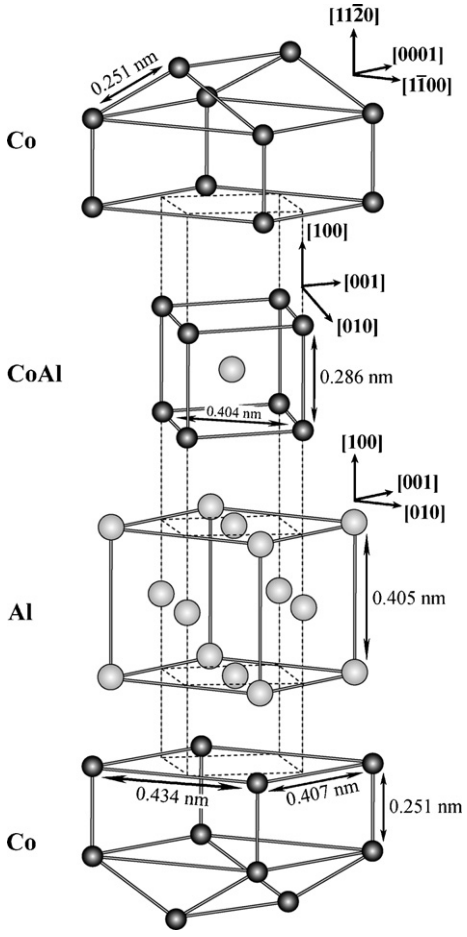

Fig. 1. Schematic diagram showing the geometric relationships among hcp Co(1 1 $\bar{2}$ 0), fcc Al(1 0 0), and B2 CoAl(1 0 0).

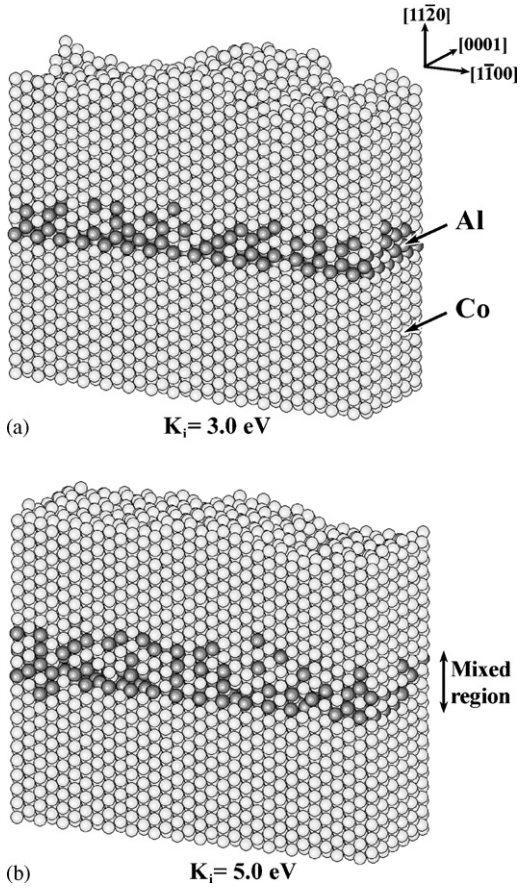

Fig. 2. Atomic configurations of Co(1 1 $\bar{2}$ 0)/CoAl/Co(1 1 $\bar{2}$ 0) multilayers fabricated with different incident energy Co adatoms: (a) 3.0 eV and (b) 5.0 eV.

For quantitative analysis of the intermixed region, the layer coverage fraction of Co and Al atoms along the [1 1 $\bar{2}$ 0] direction was calculated and the results are shown in Fig. 3. The deposition layer height was normalized to the initial surface of the Co(1 1 $\bar{2}$ 0) substrate, and 100% layer coverage corresponds to the occupancy of 192 atoms in each layer irrespective of the atom type. As can be seen in Fig. 3(a), the deposition of Co adatoms with 3.0 eV incident energy resulted in more pronounced alternating mixed layers of Co and Al in terms of layer coverage compared to the case of 5.0 eV (Fig. 3(b)). The thickness of the intermixed region was calculated to be 0.88 and 0.75 nm for K_i of 5.0 eV and K_i of 3.0 eV, respectively, and a sharp interface between the CoAl intermixed layer and the Co (1 1 $\bar{2}$ 0) film could be defined for the 3.0 eV case. In the case of the 5.0 eV deposition, the intermixed region consisted of three layers with alternating high and low Al concentrations and four intermixed layers with 20 at.% Al resulting from the displacement of Al atoms from their original positions in the surface layers in the course of deposition process.

To further investigate the structure of the intermixed region in detail, the nearest neighbor distribution, which gives the information of the exact local geometric structures at the mixed regions, was calculated. This method can analyze the structure for not only selected region but also selected atoms. Since magnetic properties of Co–Al alloy were found to be highly localized to the neighboring atoms [29], nearest-neighbor analysis adopted in this study is very suitable to investigate the local geometric structures of each atom exactly. Only information for the location of an atom was required to search for the neighboring atoms and to obtain the crystal structures. From the calculation, it could be found that the mixed regions were composed of significant amounts of bcc atoms surrounded by eight nearest neighbor atoms. Specifically, when a Co (or Al) atom is surrounded by eight Al (or Co) atoms, the bcc atom corresponds to a B2 atom. In total 1486 atoms for the case of K_i 3.0 eV and 1640 atoms for K_i 5.0 eV contributed to the mixing layer. Among them 59.5 and 40.1% of total atoms could be identified as bcc atoms for 3.0 and 5.0 eV, respectively.

Fig. 4 shows the calculated results for the BCC fraction as a function atomic percent Co. It can be clearly seen that various compositions of Co_xAl_{1-x} structures were formed in the mixed region according to the deposition conditions. In the case of 3.0 eV incident energy, the Co adatoms penetrated and mixed less actively with the Al atoms compared to the 5.0 eV case. Therefore, instead of a perfect B2 CoAl structure, a bimodal distribution of Co_xAl_{1-x} structures with Co or Al rich compositions was present. On the other hand, in the 5.0 eV case, a significant amount of B2 CoAl and Co_xAl_{1-x} ($x = 0.812$) structures could be seen in the mixed region. It can be reasonably inferred that

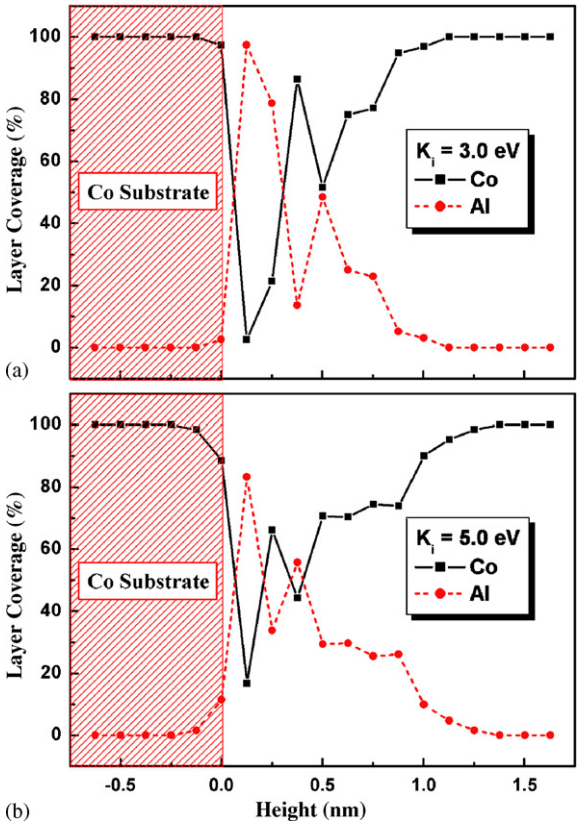

Fig. 3. Layer coverage fraction of Co(1 1 $\bar{2}$ 0)/CoAl/Co(1 1 $\bar{2}$ 0) multilayers fabricated with different incident energy Co adatoms: (a) 3.0 eV and (b) 5.0 eV.

Co atoms with 5.0 eV K_i could penetrate deeper and mix more readily with Al atoms. Interestingly, the existence of a zone of 20 at.% Al in the intermixed region, confirmed in Fig. 3(b), is consistent with the presence of a Co_xAl_{1-x} ($x = 0.812$) structure.

The structural configurations are illustrated graphically in Fig. 5 after a filtering process in which each atomic structure was distinctively represented by shades of gray. It can be seen that a mixed region composed of bcc atoms could be clearly observed for both deposition conditions, 3.0 and 5.0 eV. Consequently, sharp interfaces of Co(1 1 $\bar{2}$ 0)/Co_xAl_{1-x}, and Co_xAl_{1-x}/Co(1 1 $\bar{2}$ 0) can be seen in Fig. 5.

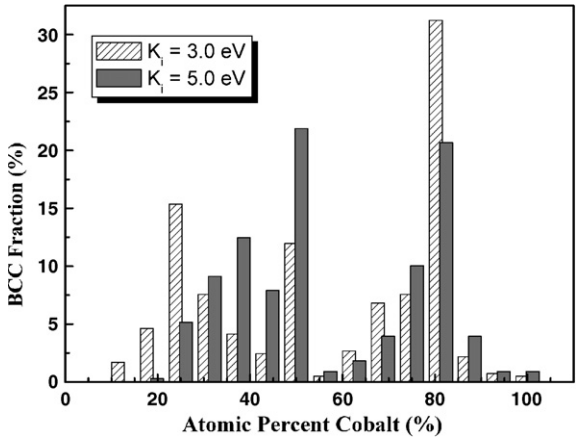

Fig. 4. Distributions of Co_xAl_{1-x} compositions in the intermixed region.

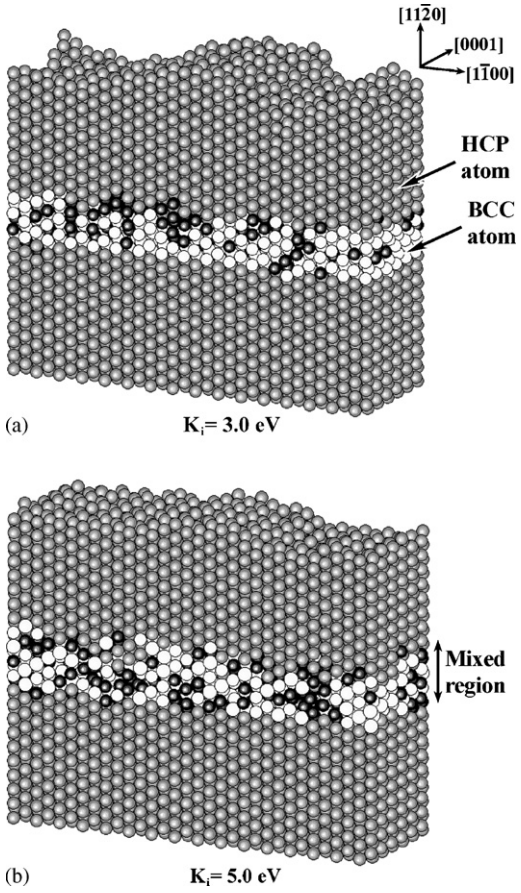

Fig. 5. Structural configurations of Co(1 1 $\bar{2}$ 0)/CoAl/Co(1 1 $\bar{2}$ 0) multilayers fabricated with incident energies of: (a) 3.0 eV and (b) 5.0 eV. (Black atoms represent defective atoms not belonging to bcc or hcp.)

4. Conclusions

Based on the molecular dynamics simulation, the multilayer system of Co(1 1 $\bar{2}$ 0)/Co_xAl_{1-x}/Co(1 1 $\bar{2}$ 0) was simulated and the corresponding quantitative atomic and structural analyses were performed. Due to the large difference in the activation energy barrier for the incorporation of adatoms in the Co/Al and Al/Co cases, a sharp interface could be obtained for the case of Al atoms deposited on a Co(1 1 $\bar{2}$ 0) substrate and a well ordered fcc Al(1 0 0) films grew on Co(1 1 $\bar{2}$ 0). On subsequent deposition of Co atoms with 3.0 and 5.0 eV incident energy on the grown Al(1 0 0) thin films, the Al film apparently disappeared and was replaced by alternating mixed layers of Co and Al. From the structural analysis, Co_xAl_{1-x} structures of various compositions were found to be formed in the mixed region and sharp interfaces were distinctly observed for the Co(1 1 $\bar{2}$ 0)/Co_xAl_{1-x}, and Co_xAl_{1-x}/Co(1 1 $\bar{2}$ 0) systems.

References

[1] J. Enkovaara, A. Ayuela, R.M. Nieminen, Phys. Rev. B 62 (2000) 16018–16022.
[2] J.M. Pruneda, R. Robles, S. Bouarab, J. Ferrer, A. Vega, Phys. Rev. B 65 (2001) 0244401–0244405.

[3] H. Ardhuin, E. Snoeck, M.-J. Casanove, J. Crystal Growth 182 (1997) 394–402.
[4] A. Wiessner, M. Agne, D. Reuter, J. Kirchner, Surf. Sci. 377–379 (1997) 937–942.
[5] S. Oikawa, A. Shibata, S. Iwata, S. Tsunashima, J. Magn. Magn. Mater. 177–181 (1998) 1273–1274.
[6] B. Benaissa, P. Humbert, H. Lefakis, J. Werckmann, V.S. Speriosu, B.A. Gurney, J. Magn. Magn. Mater. 148 (1995) 15–16.
[7] J.M. de Teresa, A. Barthélémy, A. Fert, J.P. Contour, F. Montaigne, P. Seneor, Science 286 (1999) 507–509.
[8] S.-P. Kim, Y.-C. Chung, S.-C. Lee, K.-R. Lee, K.-H. Lee, J. Appl. Phys. 93 (2003) 8564–8566.
[9] S.-P. Kim, S.-C. Lee, K.-R. Lee, Y.-C. Chung, Jpn. J. Appl. Phys. 43 (2004) 3818–3821.
[10] S.-P. Kim, S.-C. Lee, K.-R. Lee, Y.-C. Chung, J. Kor. Phys. Soc. 44 (2004) 18–21.
[11] C. Kim, Y.-C. Chung, J. Kor. Phys. Soc. 45 (2004) 1210–1213.
[12] G.W. Anderson, P.R. Norton, Surf. Sci. 336 (1995) 262–268.
[13] I. Klik, U.M. Chen, Y.D. Yao, C.K. Lo, C.P. Chang, S.Y. Liao, Y. Liou, Appl. Surf. Sci. 113/114 (1997) 165–168.
[14] J.C.A. Huang, Y. Liou, H.L. Liu, Y.J. Wu, J. Crystal Growth 139 (1994) 363–371.
[15] E. Hueger, H. Wormeester, E. Bauer, Surf. Sci. 438 (1999) 185–190.
[16] M. Tanaka, N. Ikarashi, H. Sakakibara, K. Ishida, T. Nishinaga, Appl. Phys. Lett. 60 (1992) 835–837.
[17] N. Maeda, M. Kawashima, Y. Horikoshi, J. Appl. Phys. 78 (1995) 6013–6026.
[18] J.Y. Rhee, Y.V. Kudryavtsev, K.W. Kim, Y.P. Lee, J. Appl. Phys. 87 (2000) 5887–5889.
[19] Q.S. Bie, M. Lu, J. Du, H.W. Zhao, K. Xia, H.R. Zhai, S.M. Zhou, Q.Y. Jin, L.Y. Chen, Phys. Lett. A 210 (1996) 341–346.
[20] T. Mitsuzuka, A. Kamijo, H. Igarashi, J. Appl. Phys. 68 (1990) 1787–1790.
[21] M.S. Daw, M.I. Baskes, Phys. Rev. Lett. 50 (1983) 1285–1288.
[22] R. Pasianot, E.J. Savino, Phys. Rev. B 45 (1992) 12704–12710.
[23] A. Voter, S. Chen, Mater. Res. Soc. Symp. Proc. 82 (1987) 175–180.
[24] C. Vailhé, D. Farkas, J. Mater. Res. 12 (1997) 2559–2570.
[25] G. Simmons, H. Wang, Single Crystal Elastic Constants and Calculated Aggregate Properties, MIT Press, Cambridge, Massachusetts, 1977.
[26] P. Villas, L. Calvert, Pearson's Handbook of Crystallographic Data for Intermetallic Phases, second ed., ASM International, Materials Park, OH, 1991.
[27] X.W. Zhou, R.A. Johnson, H.N.G. Wadley, Acta Mater. 45 (1997) 4441–4452.
[28] J. Rifkin, XMD Molecular Dynamics Program, University of Connecticut, 2002.
[29] S.-P. Kim, Y.-C. Chung, IEEE Trans. Magn. 41 (2005) 3343–3345.